

## Article

# A Quantitative Reconstruction of Nutrient Changes of Quaternary Red Soils (Luvisols) Affected by Land-Use Patterns

Ying-Ying Jiang <sup>1</sup>, Zhong-Xiu Sun <sup>2,\*</sup>, Ruo-Meng Wang <sup>2</sup>, Hong-Ling Wang <sup>1</sup> and Jia-Qing Wang <sup>1,\*</sup>

<sup>1</sup> College of Life Engineering, Shenyang Institute of Technology, Shenyang Reform and Innovation Demonstration Zone, Shenyang 113122, China; yingying9111@126.com (Y.-Y.J.); wanghongling@situ.edu.cn (H.-L.W.)

<sup>2</sup> College of Land and Environment, Shenyang Agricultural University, Shenyang 110866, China

\* Correspondence: zhongxiusun@syau.edu.cn (Z.-X.S.); jiaqing5212@163.com (J.-Q.W.); Tel.: +86-15734005989 (Z.-X.S.)

**Abstract:** The Quaternary red soil widely distributed in China is an important arable land resource. A quantitative understanding of nutrient changes of Quaternary red soils under different land-use patterns is the necessary premise for effective regulation, management, and sustainable utilization. In this study, five typical Quaternary red soil profiles under different land-use patterns were taken as the research object in Chaoyang City, Liaoning Province, China. The results showed that: (1) Buried Quaternary red soils were minimally affected by external disturbances. The contents of nitrogen (around 0.02%), phosphorus (ranging from 0.06% to 0.07%), and potassium (ranging from 3.12% to 3.50%) were at relatively low levels and homogeneously distributed with depth. (2) The total nitrogen content of red soils under each land-use pattern showed an increasing trend in the upper part of the profile (A and B horizons), and a sequence of woodland (CL-04) > grassland (CL-03) > arable land (CL-05) = sparse forest–grassland (CL-02). The nitrogen content in the lower part of different land-use patterns was about 0.02%. The phosphorus content of the topsoil layer remained unchanged (ranging from 0.05% to 0.06%), while the subsoil phosphorus decreased to varying extents. The potassium experienced leaching in both topsoil and subsoil layers, with the topsoil losses being lower than that in the subsoil. The range of total potassium content in the grassland (CL-03) ranged from 2.64% to 4.21%, from 3.91% to 4.44% for sparse forest–grassland (CL-02), from 2.41% to 2.63% for woodland (CL-04), and 2.85% to 2.92% for arable land (CL-05), respectively. The variation in nutrient content was related to the vegetation type, coverage rate, artificial fertilization method and species, etc. The accumulative mass change in the sparse forest–grassland increased by 384.16 g/100 cm<sup>2</sup>, and the other land-use patterns showed a decreasing trend of arable land (83.71 g/100 cm<sup>2</sup>) > woodland (83.71 g/100 cm<sup>2</sup>) > grassland (83.71 g/100 cm<sup>2</sup>), with the topsoil leaching losses being smaller than those in the subsoil layer. The characteristics of windbreak, sand fixation, and soil and water conservation of the sparse forest–grassland could well hold the nutrient-rich loess sediments, resulting in increased nutrients in the Quaternary red soil, which is a reasonable land-use pattern for the Chaoyang area.

**Keywords:** soil nutrient; nutrient fluxes; horizon evolution; arable land; management



**Citation:** Jiang, Y.-Y.; Sun, Z.-X.; Wang, R.-M.; Wang, H.-L.; Wang, J.-Q. A Quantitative Reconstruction of Nutrient Changes of Quaternary Red Soils (Luvisols) Affected by Land-Use Patterns. *Agronomy* **2023**, *13*, 2386. <https://doi.org/10.3390/agronomy13092386>

Academic Editor: Yash Dang

Received: 8 August 2023

Revised: 6 September 2023

Accepted: 12 September 2023

Published: 14 September 2023



**Copyright:** © 2023 by the authors. Licensee MDPI, Basel, Switzerland. This article is an open access article distributed under the terms and conditions of the Creative Commons Attribution (CC BY) license (<https://creativecommons.org/licenses/by/4.0/>).

## 1. Introduction

Quaternary red soils have experienced intense weathering, leaching, desilication, and iron and aluminum enrichment under warm and humid climate conditions during the Early and Middle Pleistocene of the Quaternary or even earlier periods [1,2]. Quaternary red soils retain their original characteristics formed during their formation periods, as well as features derived from the combined effects of various factors such as biological and human influences [3]. Quaternary red soils are widely distributed in China, mainly in areas south of 30° N [4], and are important arable land resources. In northern regions, Quaternary red soils are mostly buried underground and are exposed to varying degrees at the surface due

to erosion and other processes. The quality of red soils varied with the influence of different land-use patterns [3]. Unscientific land use and management can decrease the Quaternary red soil quality, such as soil erosion, tillage pan formation, structural damage, and fertility decline, threatening regional agricultural and economic sustainable development [3,5]. Therefore, understanding the changes and evolution of Quaternary red soil under different land-use patterns is a prerequisite for effectively regulating, managing, and sustainably utilizing red soil resources [6,7].

As an essential component of soil quality, the soil nutrient composition affects the soil ecosystem and soil quality [8]. Its distribution, form, content, transformation, and migration are influenced by natural factors such as parent material and climatic conditions, and it is also affected by human factors such as different land-use patterns [9]. Land-use patterns of human intervention directly influence the soil nutrient composition [10]. Appropriate and rational land-use patterns can improve soil nutrient composition and enhance soil resistance to external environmental factors. Conversely, irrational land-use and management can alter the earth's biogeochemical cycles [11], cause soil property and quality degradation, result in incalculable damage, and threaten the land resources on which humans depend. Therefore, a quantitative reconstruction of the changes in the nutrient composition of Quaternary red soils under different land-use patterns is of great significance for understanding the evolution of the red soil quality and its regulation and management.

Quaternary red soils are widely distributed in China. In southern China, the area of Quaternary red soils is more than  $101.87 \times 10^4$  km<sup>2</sup>, which has been studied deeply. The total area of Quaternary red soils in northern China is 1013 km<sup>2</sup>, which has been poorly studied. Chaoyang City in Liaoning Province, a low-lying hilly area with a wide distribution of Quaternary red soils, was selected as the typical research area for this study. The soil reconstruction model was used to study the evolution of Quaternary red soils under different land-use patterns. The research results will provide a theoretical basis for agricultural production practice in the Quaternary red soil distribution area.

## 2. Materials and Methods

### 2.1. The Study Area

The Quaternary red soil widely distributed area, Beipiao, Chaoyang City, Liaoning Province in northeast China (Figure 1), was selected by observing field investigation results and consulting the China Soil Series, Liaoning Volume, and Liaoning Soil. It is a mountainous and hilly area and is located in the transition between the Inner Mongolia Plateau and the eastern coastal plain [12]. The area has been influenced by a northern temperate continental monsoon, with a current average temperature of 5.4–8.7 °C and a current annual precipitation of 450–580 mm [13,14]. The Quaternary red soil can be classified as Argosols, Alfisols, and Luvisols in the Chinese Soil Taxonomy [15], Soil Taxonomy [16], and the World Reference Base for Soil Resources [17], respectively. The buried Quaternary red soil (MC-02), 210 cm at depth, without the influence of the modern climate and human activities, was investigated as the reference base. It had 2.5 YR Hue, silty loam texture, blocky structure, hard consistence (dry), and showed few clay coatings and iron-manganese nodules.

### 2.2. Sample Collection and Pretreatment

Typical Quaternary red soils of sparse forest–grassland (CL-02), grassland (CL-03), woodland (CL-04), and arable land (CL-05) were collected (Figure 2). The main plants of each land-use pattern are in Table 1. They are in a relatively flat and stable part derived from the same stratum and thus share the same topography, parent material, climate, biology, and formation time with the buried Quaternary red soil (MC-02). The upper part (0–68 cm) of the MC-02 is loess, and the underlying lower part (68–210 cm) is the buried Quaternary red soil. Therefore, the underlying lower part (68–210 cm) was used as the reference base.

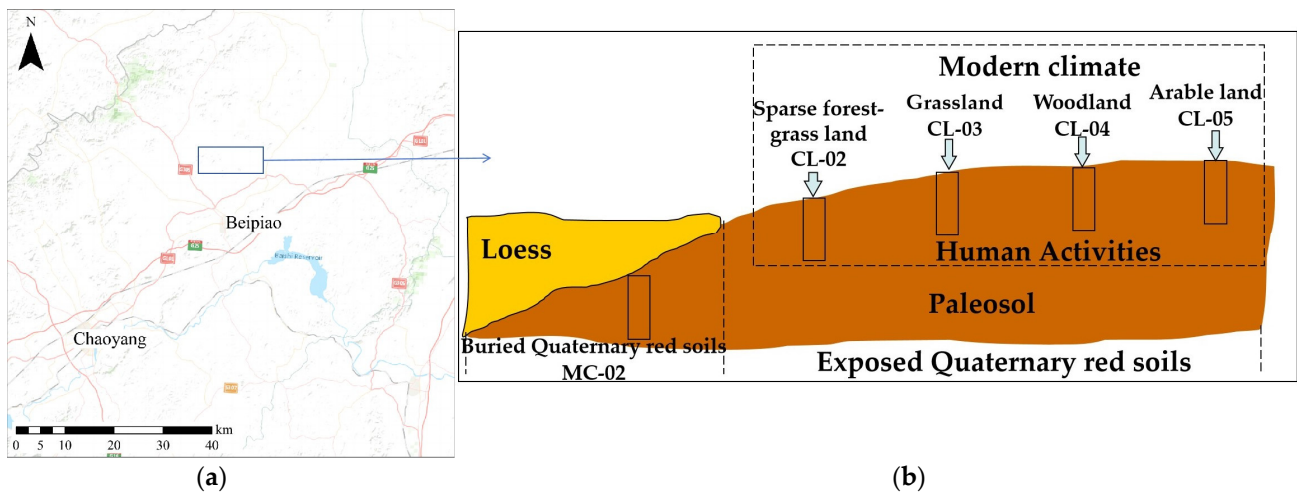


**Figure 1.** (a) The location map of Chaoyang City, Liaoning Province, China. The schematic map was plotted based on the World Topographic Map (2016) using Arc GIS 10.2.2. (b) The sampling points schematic distribution map.

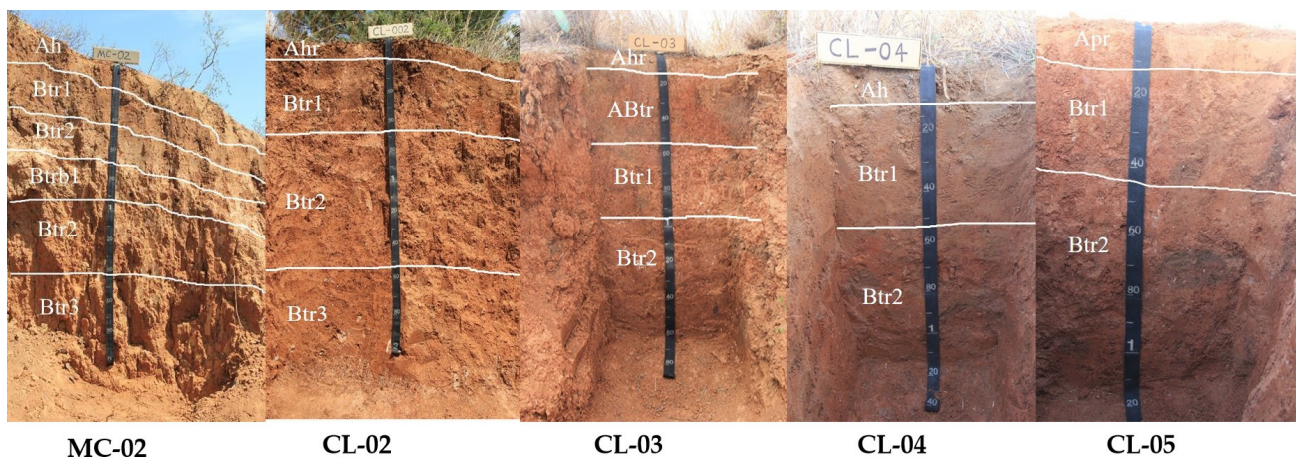


**Figure 2.** The Quaternary red soil view under different land-use patterns.

**Table 1.** The main plants of different land-use patterns.

ProfileNo.	Land-Use Patterns	Vegetation Coverage	The Main Plants
CL-02	Sparse forest-grassland	30%	The herbaceous plants: <i>Themeda triandra</i> Forssk. The woody plants: <i>Vitex negundo</i> var.; <i>heterophylla</i> (Franch.) Rehd., <i>Ulmus davidiana</i> var.; <i>japonica</i> (Rehd.) Nakai, and <i>Pinus tabuliformis</i> Carrière.
CL-03	Grassland	30%	The herbaceous plants: <i>Themeda triandra</i> Forssk
CL-04	Woodland	35%	The woody plants: <i>Vitex negundo</i> var.; <i>heterophylla</i> (Franch.) Rehd.; <i>Ulmus davidiana</i> var.; <i>japonica</i> (Rehd.) Nakai, and <i>Pinus tabuliformis</i> Carrière.
CL-05	Arable land	-	<i>Zea mays</i> L.

A typical soil profile was investigated and samples from pedogenic horizons were collected under different land-use patterns. The morphologies of Quaternary red soil profiles were described according to the Manual of Soil Description and Sampling [18]. The soil samples were transported to the laboratory and airdried. The soils were also sieved through 100 mesh for upcoming analysis. The investigated profiles were derived from loess and determined to have a parent material uniformity [3].

### 2.3. Laboratory Methods

#### 2.3.1. Soil Total Nitrogen

The 0.04–0.05 g 100 mesh soil sample was first packed and compacted, and measured by an elemental analyzer produced by the Elementar Analysensysteme (Vario EL III, Elementar Company, Langensfeld, Germany) for the soil total nitrogen content (%) [19].

#### 2.3.2. Soil Total Phosphorus and Total Potassium

The 0.25 g 100 mesh soil sample was thoroughly mixed with 2 g sodium hydroxide in the nickel crucible. Then, it was put into a high-temperature electric furnace and melted at 720 °C for 15 min. The melt material was finally dissolved and made up to 100 mL volumetric bottle for the determination of the total phosphorus [20] and total potassium [21].

### 2.4. Soil Quantitative Reconstruction Model

The soil reconstruction model (SR) was used to quantitatively calculate gains or losses of a specific component in a volume of 100 cm<sup>3</sup> of a weathered soil layer during pedogenesis [22]. The reconstruction results of a specific component in the unit area can be quantitatively compared with each other. The unit volume factor (UVF) can describe the changes in soil volume.

The equations are as follows.

$$UVF = \frac{BD_w \times C_{iw}}{BD_{pm} \times C_{ipm}} \quad (1)$$

$$D_{jw} = BD_w \times C_{jw} - UVF \times (BD_{pm} \times C_{jpm}) \quad (2)$$

Note:  $BD_w$  represents the bulk density of a weathered soil layer;  $BD_{pm}$  represents the bulk density of the parent material of the weathered soil layer;  $C_{iw}$  represents the content of a stable, referenceable component in the weathered soil layer;  $C_{ipm}$  represents the content of a stable, referenceable component  $i$  in the parent material;  $C_{jw}$  represents the content of component  $j$  in the weathered soil layer;  $C_{jpm}$  represents the content of component  $j$  in the parent material of the weathered soil layer;  $D_{jw}$  represents the change in the content of component  $j$  in the weathered soil layer during pedogenesis.

### 2.5. Data Processing and Analysis

The Descriptive Statistics and Calculated Variable in SPSS Statistics 17.0 were used for data statistics. The SigmaPlot 12.5 was used for plotting graphs.

## 3. Results

The buried red soil has a Hue of 2.5 YR, a value of 6 to 7, and a Chroma of 6 to 8. It has a silty loam texture, blocky structure, hard consistency in dry conditions, a few clay coatings, and iron–manganese nodules. These morphologies distribute uniformly with depth. Compared to the buried red soil, exposed red soils under different land-use patterns have similar structure and consistency, while their color and texture slightly vary with depth. Their topsoil (A horizon) and subsoil (B horizon) increase to 5 YR in Hue, with a darkening value between 4 and 6. The texture of red soils under the sparse forest–grassland, grassland, and forestland varies from silty loam to silt clay loam/clay loam with depth, while arable land remains unchanged and distributes uniformly for silty

loam with depth. The morphology in terms of color and texture can relate to changes in total nitrogen content, phosphorus content, and potassium content with soil depth. The darkening color showed by value and finer texture relates to increased total nitrogen, unchanged phosphorus, and decreased potassium content, and also relates to their fluxes showing complex nonlinearity relationships.

### 3.1. Distribution Characteristics of the Total Nitrogen in Quaternary Red Soils under Different Land-Use Patterns

The nitrogen content of the buried Quaternary red soil (MC-02) is around 0.02% and homogeneously distributed with depth. The buried Quaternary red soils were exposed at the surface, and affected by different land-use patterns, resulting in significant changes in the soil's total nitrogen content within the profile. The soil total nitrogen in woodland (CL-04) and grassland (CL-03) varied greatly, ranging from 0.027% to 0.158% and 0.017% to 0.078%, respectively. The arable land (CL-05) and sparse forest–grassland (CL-02) have relatively smaller ranges of soil total nitrogen, from 0.019% to 0.057% and 0.018% to 0.055% (Figure 3), respectively. The total nitrogen content of Quaternary red soils under different land-use patterns showed a decreasing trend with depth. However, the total nitrogen content of red soils under each land-use pattern showed an increasing trend in the upper part of the profile (A and B horizons), and a sequence of woodland (CL-04) > grassland (CL-03) > arable land (CL-05) = sparse forest–grassland (CL-02). The nitrogen content in the lower part of different land-use patterns was about 0.02%, which was basically consistent with the buried Quaternary red soil (Figure 3).

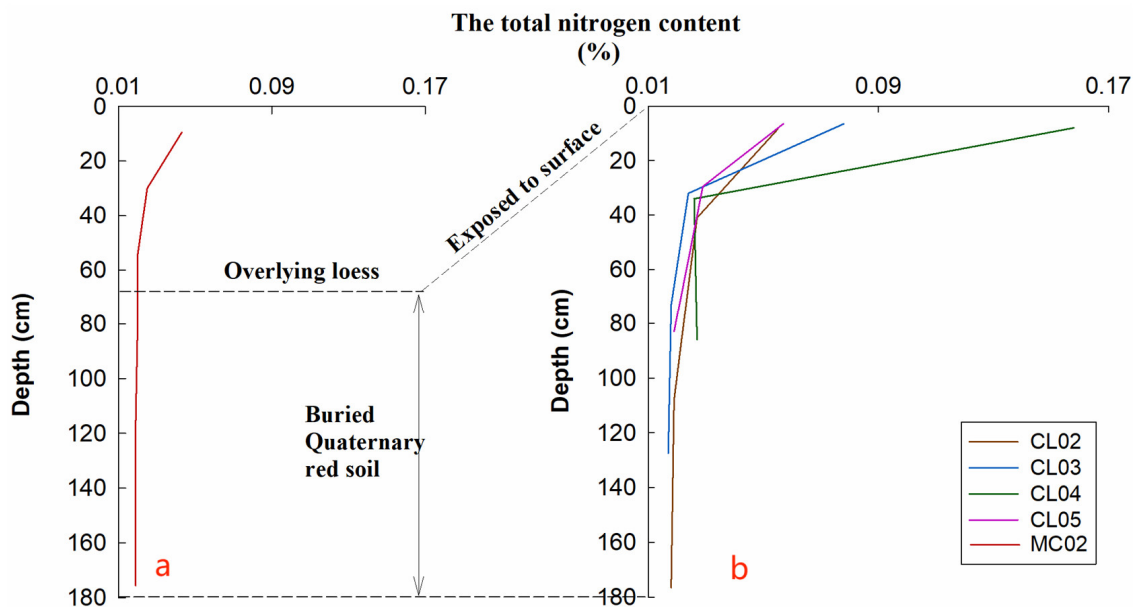


**Figure 3.** Distribution characteristics of the soil total nitrogen in Quaternary red soils. (a) Buried Quaternary red soil; (b) exposed Quaternary red soils under different land-use patterns.

### 3.2. Distribution Characteristics of the Total Phosphorus in Quaternary Red Soils under Different Land-Use Patterns

The total phosphorus content in buried Quaternary red soils (MC-02) did not change significantly with the depth, ranging from 0.06% to 0.07%. The total phosphorus content under different land-use patterns changed slightly, ranging from 0.05% to 0.06%, which was greater than that of the buried Quaternary red soil. The total phosphorus content of red soils under different land-use patterns showed that the upper part was greater than the lower part (Figure 4).

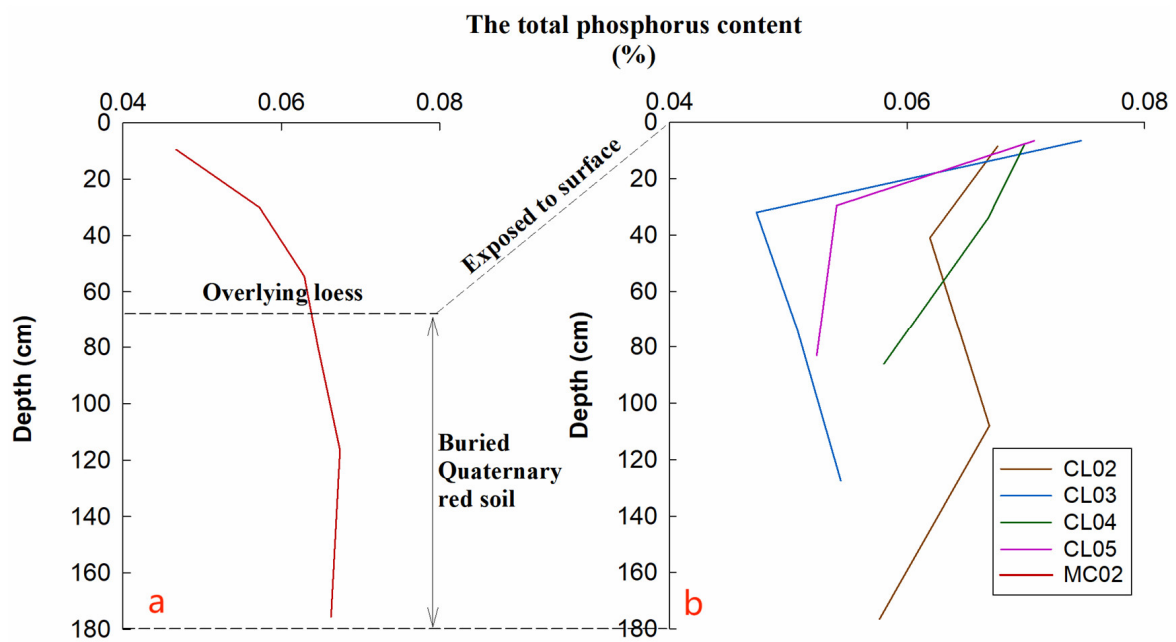


**Figure 4.** Distribution characteristics of the total phosphorus in Quaternary red soils. (a) Buried Quaternary red soil; (b) exposed Quaternary red soils under different land-use patterns.

*3.3. Distribution Characteristics of the Total Potassium in Quaternary Red Soils under Different Land-Use Patterns*

The potassium content in the buried Quaternary red soils (MC-02) first increased and then decreased with soil depth, ranging from 3.12% to 3.50% (Figure 5). The potassium content in the soil below 120 cm was uniformly distributed with a depth of 3.12%. The range of total potassium content in the grassland (CL-03) was the largest, ranging from 2.64% to 4.21%. The content of total potassium in sparse forest–grassland (CL-02) varied from 3.91% to 4.44%. The total potassium content of the other two land-use patterns was smaller than that of the buried Quaternary red soil, which ranged from 2.41% to 2.63% for woodland (CL-04) and 2.85% to 2.92% for arable land (CL-05), respectively (Figure 5).

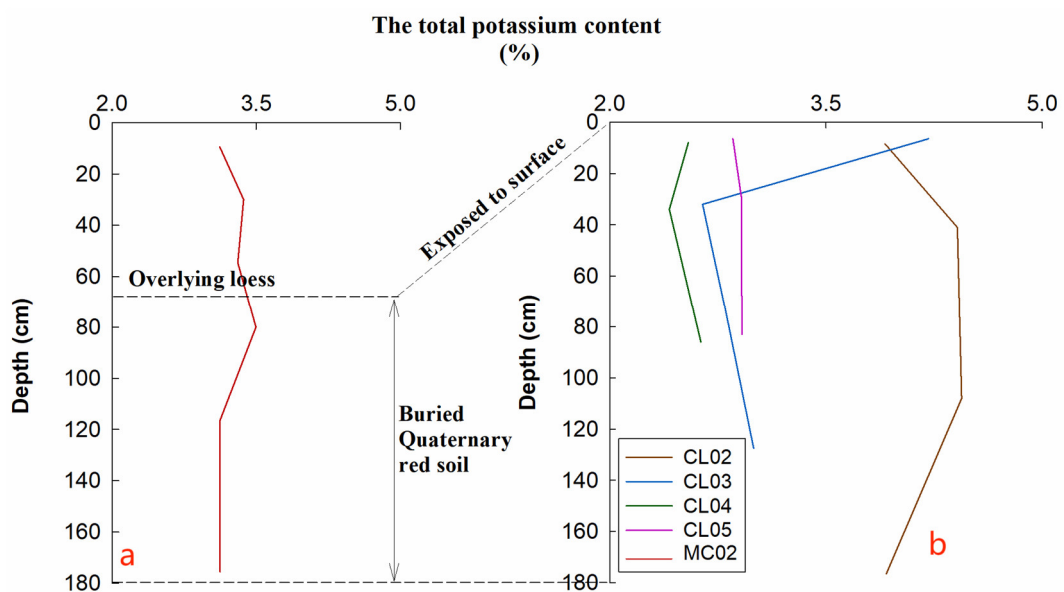


**Figure 5.** Distribution characteristics of the total potassium in Quaternary red soils. (a) Buried Quaternary red soil; (b) exposed Quaternary red soils under different land-use patterns.

### 3.4. Results of the SR Model

Compared with the buried Quaternary red soils (MC-02), the soil nitrogen content in profiles under different land-use patterns had increased in the surface layer (layer A). Among them, the woodland (CL-04) had the largest increase, with  $0.19 \text{ g}/100 \text{ cm}^3$ . The increase in sparse forest–grassland (CL-02), grassland (CL-03), and arable land (CL-05) was smaller, which were  $0.05 \text{ g}/100 \text{ cm}^3$ ,  $0.07 \text{ g}/100 \text{ cm}^3$ , and  $0.06 \text{ g}/100 \text{ cm}^3$ , respectively. There was almost no change in the soil total nitrogen of subsoil layers (B layer). The soil phosphorus content in subsoil layers (layer B) under different land-use patterns reduced by  $0.01 \text{ g}/100 \text{ cm}^3$ – $0.03 \text{ g}/100 \text{ cm}^3$ . The soil potassium content varied greatly under different land-use patterns, among which the overall potassium content in the sparse forest–grassland (CL-02) increased by  $1.05 \text{ g}/100 \text{ cm}^3$  in the surface layer (A) and  $1.98 \text{ g}/100 \text{ cm}^3$  in the subsoil layer (B). The potassium content in the surface soil of the grassland (CL-03) increased by  $1.29 \text{ g}/100 \text{ cm}^3$ , while that in the subsoil decreased by  $0.56 \text{ g}/100 \text{ cm}^3$ . The changes in woodland (CL-04) were similar to the arable land (CL-05). And the potassium content in all layers showed a decreasing trend, with the surface layer decreasing by  $0.55 \text{ g}/100 \text{ cm}^3$  and  $0.53 \text{ g}/100 \text{ cm}^3$ , and the potassium content in the subsoil layer was smaller than that in the surface layer, decreasing by  $0.74 \text{ g}/100 \text{ cm}^3$  and  $0.70 \text{ g}/100 \text{ cm}^3$ , respectively.

## 4. Discussion

The soil nutrient content is an important indicator for evaluating soil fertility levels [9]. The plant growth and land productivity are limited by the soil nutrient availability [11]. The soil nutrient content can usually reflect the conditions of parent material, climate, and vegetation, and its vertical distribution can be used to explore the process of nutrient input, output, and circulation [23]. At the same time, soil nutrients can also reflect the ecosystem health [23]. Therefore, the characteristics of soil nutrients have become an important research field in pedology, agronomy, ecology, and environmental science [11,24].

### 4.1. Changes in the Total Nitrogen in Quaternary Red Soils under Different Land-Use Patterns

The soil nitrogen accumulated through the biological nitrogen fixation process and non-biological nitrogen fixation process [25]. Biological nitrogen fixation, the main nitrogen fixation, is the fixation of atmospheric molecular nitrogen into ammonia by nitrogen-fixing microorganisms in plants under normal temperature and pressure and the catalysis of corresponding enzymes, which is further transformed into amino acids and protein compounds [26]. Subsequently, with the death of plants, as residues such as fallen leaves and dead branches, nitrogen is transformed into the soil component. Different land-use types have different land cover vegetation. The types and contents of soil organic matter transformed by plant root exudates, dead leaves, and other residues lead to changes in soil microbial communities, resulting in the differentiation of soil nitrogen mineralization and transformation, thus affecting the soil nitrogen content distribution [27].

The buried Quaternary red soils (MC-02) are minimally affected by external factors (such as human activities) due to being buried, with less external nitrogen input and weaker soil microbial activity. Therefore, the nitrogen content in the buried Quaternary red soils was only about 0.02% and distributed homogeneously with depth (Figure 3). Compared with the buried Quaternary red soils, the surface of sparse forest–grassland (CL-02), grassland (CL-03), and woodland (CL-04) have plant invasion (herbs and shrubs). The external nitrogen fixed in plants returned to the soil with the death and decay of plants, thus increasing the nitrogen content in the surface soil to  $0.05 \text{ g}/100 \text{ cm}^3$ ,  $0.07 \text{ g}/100 \text{ cm}^3$ , and  $0.19 \text{ g}/100 \text{ cm}^3$ , respectively (Table 2). Although the arable land (CL-05) was covered by crops during the growing season, most of the soil nitrogen was taken away following the crop harvest. The soil surface nitrogen content increased by  $0.06 \text{ g}/100 \text{ cm}^3$ , which was caused by nitrogen input into the soil through artificial fertilization and other human activities. These land-use patterns directly affected the nitrogen content in the topsoil [27], while the subsoil layer was minimally affected. So, the subsoil nitrogen content under

different land-use patterns remained almost unchanged when compared to the buried Quaternary red soil (MC-02). The total accumulative change of soil nitrogen under different land-use patterns showed a trend of woodland (CL-04) ( $4.50 \text{ g}/100 \text{ cm}^3$ ) > sparse forest-grassland (CL-02) ( $1.48 \text{ g}/100 \text{ cm}^3$ ) > arable land (CL-05) ( $0.97 \text{ g}/100 \text{ cm}^3$ ) > grassland (CL-03) ( $0.72 \text{ g}/100 \text{ cm}^3$ ). The increase in woodland nitrogen was the largest, mainly due to its high plant coverage and a potentially large return rate. The large amounts of residues were accumulated and mineralized, which returned nutrients to the soil and improved the soil texture and moisture penetration to increase the activity of microorganisms and enhance the effect of soil nitrogen fixation [27,28]. At the same time, the root decomposition products in the soil produced acidic substances, promoting the transformation of insoluble minerals and other substances into effective nitrogen components, thus increasing the nitrogen content in the soil [28]. While the arable land and grassland had lower vegetation coverage and return rates, resulting in smaller increases of nitrogen content when compared to the buried Quaternary red soil.

**Table 2.** The quantitative reconstruction results of nutrient changes using the soil reconstruction model (SR).

Profile No.	Horizon	Depth (cm)	TN (g/100 cm <sup>3</sup> )	TP (g/100 cm <sup>3</sup> )	TK (g/100 cm <sup>3</sup> )	MC (g/100 cm <sup>3</sup> )
MC-02	2Btr2	90–100	0.00	0.00	0.00	0.00
CL-02	Ah	0–17	0.05	0.00	1.05	1.10
	Btr1	17–65	0.02	0.00	2.45	2.47
	Btr2	65–151	0.00	0.00	2.15	2.15
	Btr3	151–202	0.00	−0.02	1.24	1.22
	Variation of the layer B		0.00	−0.01	1.98	1.97
Variation of cumulative mass (g/100 cm <sup>2</sup> )			1.48	−1.02	383.70	384.16
CL-03	Ah	0–13	0.07	0.01	1.29	1.37
	BA	13–51	0.00	−0.02	−0.59	−0.61
	Btr1	51–95	0.00	−0.03	−0.77	−0.80
	Btr2	95–160	0.00	−0.02	−0.41	−0.43
	Variation of the layer B		0.00	−0.02	−0.56	−0.59
Variation of cumulative mass (g/100 cm <sup>2</sup> )			0.72	−3.49	−65.84	−68.61
CL-04	Ah	0–16	0.19	0.01	−0.55	−0.35
	Btr1	16–52	0.01	0.00	−1.14	−1.13
	Btr2	52–120	0.02	−0.01	−0.52	−0.51
	Variation of the layer B		0.01	−0.01	−0.74	−0.73
Variation of cumulative mass (g/100 cm <sup>2</sup> )			4.50	−0.56	−85.54	−81.60
CL-05	Ap	0–13	0.06	0.00	−0.53	−0.47
	Bt	13–46	0.01	−0.02	−0.38	−0.39
	Btr	46–120	0.00	−0.03	−0.84	−0.87
	Variation of the layer B		0.00	−0.03	−0.70	−0.73
Variation of cumulative mass (g/100 cm <sup>2</sup> )			0.97	−3.16	−81.52	−83.71

Note: MC indicates the mass change of total selected nutrients; TN indicates the total nitrogen; TP indicates the total phosphorus; TK indicates the total potassium.

#### 4.2. Changes in the Total Phosphorus of Quaternary Red Soils under Different Land-Use Patterns

In the primary ecosystem, the form and circulation of phosphorus in soils are affected by factors such as the parent material, climate, environment, time, and topography. During the transition from native ecosystems to systems disturbed by human factors, the form, content, and distribution of soil phosphorus were affected by the input–output of soil and by human activities [29]. There is no gaseous form of phosphorus in the soil. The main ways of soil phosphorus input are plant return, artificial application of chemical fertilizers, and organic fertilizers. Soil phosphorus output is mainly through two ways:

plant absorption and runoff infiltration. Soil structure, soil properties, vegetation coverage, slope, fertilization method, fertilizer amount, and precipitation are factors affecting soil phosphorus output [30–32]. It is difficult for phosphorus to leach down in the soil, surface runoff is the main way of soil phosphorus loss [30].

The phosphorus content of buried Quaternary red soils varied between 0.05% and 0.07% with a homogeneous change with depth due to the fact that it was barely affected by external factors such as runoff (Figure 4). After being exposed to the land surface, the phosphorus of Quaternary red soils had been changed to varying degrees by different land-use patterns. Plants absorb the necessary phosphorus for their growth from deep soil layers. Although a small portion of phosphorus was returned to the surface soil through crop residue mineralization, most of the phosphorus remained in plants and was taken away through crop harvest. Additionally, surface runoff caused a part of phosphorus leaching [33], the topsoil phosphorus remained essentially balanced under different land-use patterns. The phosphorus in the subsoil decreased due to limited leaching. The losses of subsoil showed a trend of grassland ( $3.49 \text{ g}/100 \text{ cm}^3$ ) > arable land ( $3.16 \text{ g}/100 \text{ cm}^3$ ) > sparse forest–grassland ( $1.02 \text{ g}/100 \text{ cm}^3$ ) > woodland ( $0.56 \text{ g}/100 \text{ cm}^3$ ). Due to the low vegetation coverage rate of grassland and basically no coverage of arable land after the autumn harvest, the Quaternary red soils were vulnerable to erosion caused by wind and water, resulting in relatively high phosphorus loss in the profile. The woodland with a large surface coverage and stable soil structure can hold more phosphorus in soil when compared to others.

#### 4.3. Changes in the Total Potassium in Quaternary Red Soils under Different Land-Use Patterns

Different land-use patterns lead to differences in soil physical and chemical properties and then affect the migration and transformation of potassium [34]. The main input modes of soil potassium are atmospheric dust deposition and external application of potassium fertilizers, the main output modes are leaching with the soil solution [35].

The potassium content of the buried Quaternary red soil varied between 3.12% and 3.51% and showed a homogeneous change with depth due to being hardly affected by external factors. Under different land-use patterns, potassium leaching occurred in topsoil and subsoil layers to varying degrees of Quaternary red soil profiles except for sparse forest–grassland, which had a greater loss in the subsoil than that in the topsoil. This could be explained that the potassium is highly soluble and easily migrates with soil solution, causing a large amount of potassium to leach downward out of the soil. In addition, plants absorb potassium from the subsoil layer to meet their growth and development [36]. Compared to buried Quaternary red soils, the potassium content of sparse forest–grassland increased by  $383.70 \text{ g}/100 \text{ cm}^3$ , while others showed a decreasing trend of woodland ( $85.5 \text{ g}/100 \text{ cm}^3$ ) > arable land ( $81.52 \text{ g}/100 \text{ cm}^3$ ) > grassland ( $65.84 \text{ g}/100 \text{ cm}^3$ ). The woodland had the largest loss of potassium. This may be due to the surface vegetation with a high coverage had absorbed a considerable amount of potassium from the soil, and the absorbed amount of potassium was greater than the returned amount [37]. The decrease in arable land was relatively larger, which may be due to that the crops absorbed potassium and were taken away for harvest, resulting in a very small return of soil potassium, leading to the decrease in potassium in soil [38]. At the same time, the low vegetation coverage of arable land was vulnerable to soil erosion, which was also a reason for the decrease in soil potassium [38]. As a combination of woodland and grassland, sparse forest–grassland had the characteristics of windbreak, sand fixation, and soil and water conservation, which could well hold a large amount of potassium-rich loess sediments, resulting in an increasing trend of potassium in the profile [39].

#### 4.4. The nutrient Evolution of Quaternary Red Soils under Different Land-Use Patterns

Different land-use patterns have a significant impact on the soil nutrient composition and distribution [40]. The total nutrient mass change (MC) of Quaternary red soils has decreased with a wide range, which was due to the serious soil erosion in the Chaoyang area.

Compared to the buried Quaternary red soil, total nutrients in the topsoil and subsoil layers under different land-use patterns (except for the sparse forest–grassland) have experienced different degrees of losses. The loss of the topsoil layer was lower than that of the subsoil layer. This was because some nutrients could migrate downward with the soil solution to leach out of the soil, and the lost nutrients were not replenished in time [41]. In addition, plants absorbed nutrients from deep soil, and the returned amount was less than the absorbed amount, which was also a reason for the decrease in soil nutrients. Although fertilization would supply some nutrients in arable land, the applied fertilizer generally compounds fertilizer and organic fertilizer and does not provide a specific supplement for a specific element in soil. At the same time, soil erosion would also aggravate the nutrient leaching. The surface vegetation of the sparse forest–grassland consisted of woody and herbaceous plants, which could effectively prevent wind erosion, stabilize the sand, conserve water and soil, and efficiently retain nutrient-rich loess deposits in the soil. As a result, the accumulative mass change in sparse forest–grassland increased by 384.16 g/100 cm<sup>2</sup>. However, the cumulative mass change of other land-use patterns showed a decreasing trend of arable land (83.71 g/100 cm<sup>2</sup>) > woodland (83.71 g/100 cm<sup>2</sup>) > grassland (83.71 g/100 cm<sup>2</sup>).

## 5. Conclusions

Different land-use patterns can cause the redistribution of soil nutrients by affecting surface vegetation status and soil microbial species, etc., thus affecting land productivity and soil quality. Therefore, the quantitative research on the evolution characteristics of soil nutrients under different land-use patterns is of great significance for selecting and optimizing land-use patterns and improving soil productivity and land management levels.

(1) The buried Quaternary red soil was minimally affected by external disturbances. The contents of nitrogen, phosphorus, and potassium were at relatively low levels and homogeneously distributed with depth.

(2) Compared to the buried Quaternary red soil, the topsoil nitrogen content of Quaternary red soils increased under different land-use patterns, while the subsoil nitrogen content remained relatively stable. The phosphorus content of the topsoil layer remained unchanged, while the subsoil phosphorus decreased to varying extents. The potassium experienced leaching in both topsoil and subsoil layers, with the topsoil losses being lower than that in the subsoil.

(3) The variation in nutrient content was related to the vegetation type, coverage rate, artificial fertilization method, species, etc.

(4) Compared to the buried Quaternary red soil, their daytime counterparts showed different degrees of nutrient leaching loss in both topsoil and subsoil layers except for the sparse forest–grassland, with the topsoil leaching losses being smaller than those in the subsoil layer.

(5) The characteristics of windbreak, sand fixation, and soil and water conservation of sparse forest–grassland could well hold the nutrient-rich loess sediments, resulting in increased nutrients, which is a reasonable land-use pattern in the Chaoyang area.

**Author Contributions:** Conceptualization, Y.-Y.J., Z.-X.S. and J.-Q.W.; Data Curation, Y.-Y.J. and Z.-X.S.; Formal Analysis, Y.-Y.J., Z.-X.S. and R.-M.W.; Funding Acquisition, Y.-Y.J., Z.-X.S., H.-L.W. and J.-Q.W.; Investigation, Y.-Y.J. and Z.-X.S.; Methodology, Y.-Y.J., Z.-X.S. and R.-M.W.; Project Administration, Y.-Y.J. and Z.-X.S.; Resources, Y.-Y.J. and Z.-X.S.; Software, Y.-Y.J., Z.-X.S. and J.-Q.W.; Supervision, Y.-Y.J. and Z.-X.S.; Validation, Y.-Y.J., Z.-X.S., H.-L.W. and J.-Q.W.; Visualization, Y.-Y.J. and Z.-X.S.; Writing—Original Draft, Y.-Y.J., Z.-X.S., R.-M.W. and J.-Q.W.; Writing—Review and Editing, Y.-Y.J., Z.-X.S. and J.-Q.W. All authors have read and agreed to the published version of the manuscript.

**Funding:** This research was funded by the Applied Basic Research Program of Liaoning Province (No. 2022JH2/101300167), the National Natural Science Foundation of China (No. 42277285), the Basic Scientific Research Project of Liaoning Provincial Department of Education (No. LJKZ1341), and the Applied Basic Research Program of Liaoning Province (No. 2023020244-JH2/1016).

**Data Availability Statement:** All data are true, valid, and can be made available.

**Acknowledgments:** The authors sincerely thank all the students and staff who provided input to this study. Our acknowledgments also extend to the anonymous reviewers for their constructive reviews of the manuscript.

**Conflicts of Interest:** The authors declare no conflict of interest. The funders had no role in the design of the study; in the collection, analyses, or interpretation of data; in the writing of the manuscript; or in the decision to publish the results.

## References

1. Wang, D.P.; Wang, Q.B.; Han, C.L.; Wang, H.Q.; Liu, S.H. Study on fractal features of paleosol in Liaoning Province. *J. Anhui Agric. Sci.* **2007**, *35*, 6186–6189.
2. Han, C.L.; Wang, Q.B.; Sun, F.J.; Liu, S.H.; Chen, H. Properties and taxonomy of Quaternary paleo-latosol-like soils in Chaoyang area of Liaoning province. *Acta Pedol. Sin.* **2010**, *47*, 836–846.
3. Duan, S.Y.; Sun, Z.X.; Wang, Q.B.; Jiang, Y.Y.; Sun, F.J. Comparison of aggregate composition in quaternary red soil under different land use patterns. *Chin. J. Soil Sci.* **2020**, *51*, 587–596.
4. Sun, Z.X.; Owens, R.P.; Han, C.L.; Chen, H.; Wang, X.L.; Wang, Q.B. A quantitative reconstruction of a loess–paleosol sequence focused on paleosol genesis: An example from a section at Chaoyang, China. *Geoderma* **2016**, *266*, 25–39. [[CrossRef](#)]
5. Duan, S.Y.; Sun, Z.X.; Wang, Q.B.; Jiang, Y.Y.; Han, C.L.; Zhang, Y.W.; Lv, M.F.; Sun, F.J.; Chen, L.M. Characteristics of soil organic carbon distribution of quaternary red soils under different land use patterns. *Chin. J. Soil Sci.* **2021**, *52*, 1078–1084.
6. Wang, Q.B.; Han, C.L. Discussion on the Status of Plaeo-latosol-like Soils in the Chinese Soil Taxonomy. *J. Shenyang Agric. Uni.* **2008**, *39*, 3–6.
7. Sun, Z.X.; Jiang, Y.Y.; Wang, Q.B.; Owens, R.P. A fractal evaluation of particle size distributions in an eolian loess-paleosol sequence and the linkage with pedogenesis. *Catena* **2018**, *165*, 80–91. [[CrossRef](#)]
8. Zhou, J.M.; Shen, R.F. *Dictionary of Soil Science*; Science Press: Beijing, China, 2013.
9. Anne, K.; Tambet, K.; Priit, P.; Ain, K. Modeling topsoil phosphorus-From observation-based statistical approach to land-use and soil based high-resolution mapping. *Agronomy* **2023**, *13*, 1183.
10. Alatengxihuri; Zeng, X.B.; Bai, L.Y.; Li, L.F.; Sun, N.; Gao, J. Effect of different land use on farmland soil nutrients. *Res. Agric. Mod.* **2010**, *31*, 492–495.
11. Zhang, J.; Li, Z.; Luo, Y.; Wang, X.; Yang, D.; Zhang, X. Thickness of a Compost Layer on the Distribution of water and nutrients in a Surface-Drip-Irrigated Sandy Soil Column. *Agronomy* **2023**, *13*, 1181. [[CrossRef](#)]
12. Han, C.L.; Liu, S.H.; Wang, Q.B.; Wang, H.Q. Basic properties and genetic characteristic research of Quaternary paleosol in Chaoyang city of Liaoning. *Chin. J. Soil Sci.* **2009**, *6*, 1233–1239.
13. Sui, J.Y. Analysis on precipitation features during the flood season of Chaoyang in Liaoning Province in recent 58 Years. *J. Anhui Agric. Sci.* **2011**, *39*, 14931–14932.
14. Zhang, F.M.; Zong, Y.F. The characteristics of temperature change in Chaoyang area of Liaoning Province. *Anhui Agric. Sci. Bull.* **2015**, *21*, 150–160.
15. Chinese Soil Taxonomy Research Group, Institute of Soil Science Chinese Academy of Sciences; Cooperative Research Group on Chinese Soil Taxonomy. *Keys to Chinese Soil Taxonomy*, 3rd ed.; University of Science and Technology of China Press: Hefei, China, 2001. (In Chinese)
16. Soil Survey Staff. *Keys to Soil Taxonomy*, 12th ed.; United States Department of Agriculture (USDA), Natural Resources Conservation Service (NRCS), U.S. Government Printing Office: Washington, DC, USA, 2014.
17. IUSS Working Group WRB. *World Reference Base for Soil Resources 2014, Update 2015 International Soil Classification System for Naming Soils and Creating Legends for Soil Maps*; World Soil Resources Reports No. 106; Food and Agriculture Organization (FAO): Rome, Italy, 2015.
18. Zhang, G.L.; Li, D.C. *Manual of Soil Description and Sampling*; Science Press: Beijing, China, 2017. (In Chinese)
19. Li, J.W.; Jiao, X.G.; Sui, Y.Y.; Cheng, S.J. The Belonging of Dark Brown Soil in the East of Jilin Province in Chinese Soil Taxonomy. *Chin. Agric. Sci. Bull.* **2011**, *27*, 74–79.
20. GB/T 9837-88; Determination of Soil Total Phosphorus. Standards Press of China: Beijing, China, 1988.
21. GB/T 9836-88; Determination of Soil Total Potassium. Standards Press of China: Beijing, China, 1988.
22. Stolt, M.H.; Baker, J.C. Quantitative comparison of soil and saprolite genesis: Examples from the Virginia Blue Ridge and Piedmont. *Southeast. Geol.* **2000**, *39*, 129–150.
23. Manuel, D.B.; Fernando, T.M.; Gallardo, A.; Bowker, M.A. Decoupling of soil nutrient cycles as a function of aridity in global drylands. *Nature* **2013**, *502*, 672–676.
24. Brewer, R. *Fabric and Mineral Analysis*; Robert, E., Ed.; Krieger Publishing Company: New York, NY, USA, 1976.
25. Kahmen, A.; Buchmann, W.N. Foliar  $\delta^{15}\text{N}$  values characterize soil N cycling and reflect nitrate or ammonium preference of plants along a temperate grassland gradient. *Oecologia* **2008**, *156*, 861–870. [[CrossRef](#)]
26. Dorji, T.; Field, D.J.; Odeh, I.O. Soil Aggregate Stability and Aggregate associated Organic Carbon under different Land Use/Land Cover Types. *Soil Use Manag.* **2020**, *36*, 308–319. [[CrossRef](#)]

27. Richter, D.D.; Markewitz, D.; Wells, C.G.; Allen, H.L.; April, R.; Heine, P.R.; Urrego, B. Soil chemical change during three decades in an old-field loblolly pine (*Pinus taeda* L.) ecosystem. *Ecology* **1994**, *75*, 1463–1473. [[CrossRef](#)]
28. Maithani, K.; Arunachalam, A.; Tripathi, R.S.; Pandey, H.N. Nitrogen mineralization as influenced by climate, soil and vegetation in a subtropical humid forest in northeast India. *For. Ecol. Manag.* **1998**, *109*, 91–101. [[CrossRef](#)]
29. Debicka, M.; Jamroz, E.; Bekier, J.; Ćwieląg-Piasecka, I.; Kocowicz, A. The Influence of Municipal Solid Waste Compost on the Transformations of Phosphorus Forms in Soil. *Agronomy* **2023**, *13*, 1234. [[CrossRef](#)]
30. Correll, D.L. The role of phosphorus in the eutrophication of receiving water: A review. *J. Environ. Qual.* **1998**, *27*, 261–266. [[CrossRef](#)]
31. Daniel, T.C.; Sharpley, A.N.; Lemunyon, J.L. Agricultural phosphorus and eutrophication: A symposium overview. *J. Environ. Qual.* **1998**, *27*, 251–257. [[CrossRef](#)]
32. Gburek, W.J.; Sharpley, A.N. Hydrologic controls on phosphorus loss from upland agricultural watersheds. *J. Environ. Qual.* **1998**, *27*, 267–277. [[CrossRef](#)]
33. Jiang, Y.Y.; Sun, Z.X.; Owens, P.R.; Adhikari, K.; Wang, Q.B.; Dorantes, M.J.; Libohova, Z. Spatial distribution of soil phosphorus, calcium, and pH after long-term broiler litter application. *J. Environ. Qual.* **2019**, *48*, 594–602. [[CrossRef](#)]
34. Tesfahunegn, G.; Gebru, T. Variation in soil properties under different cropping and other land-use systems in Dura catchment, Northern Ethiopia. *PLoS ONE* **2020**, *15*, e0222476. [[CrossRef](#)] [[PubMed](#)]
35. Negasa, T.; Ketema, H.; Legesse, A.; Sisay, M.; Temesgen, H. Variation in soil properties under different land use types managed by smallholder farmers along the toposequence in Southern Ethiopia. *Geoderma* **2017**, *290*, 40–50. [[CrossRef](#)]
36. Burst, M.; Chauchard, S.; Dambrine, E.; Dupouey, J.L.; Amiaud, B. Distribution of soil properties and forest-grassland interfaces: Influence of permanent environmental factors or land-use after-effects. *Agric. Ecosyst. Environ.* **2020**, *289*, 106739. [[CrossRef](#)]
37. Reitemeier, R.F. Soil Potassium. *Adv. Agron.* **1951**, *3*, 113–164.
38. Li, W.; Liu, X.-M.; Hu, Y.; Teng, F.Z.; Chadwick, O.A. Potassium isotope fractionation during chemical weathering in humid and arid Hawaiian regoliths. *Geochim. Cosmochim. Acta* **2022**, *333*, 39–55. [[CrossRef](#)]
39. Jiang, T. Study on the Effect of Sand Fixation and Soil Improvement by Different Land Use Methods in the Sand-Blown Area of Northwest Liaoning Province. Master's Thesis, Chinese Academy of Agricultural Sciences (CAAS), Beijing, China, 2012; pp. 1–29.
40. Zhao, W.; Huang, L. Stoichiometric characteristics and influencing factors of soil nutrients under different land use types in an alpine mountain region. *Acta Ecol. Sin.* **2022**, *42*, 4415–4427.
41. Fentie, S.F.; Jembere, K.; Fekadu, E.; Wasie, D. Land Use and Land Cover Dynamics and Properties of Soils under Different Land Uses in the Tejibara Watershed, Ethiopia. *Sci. World J.* **2020**, *2020*, 1479460. [[CrossRef](#)] [[PubMed](#)]

**Disclaimer/Publisher's Note:** The statements, opinions and data contained in all publications are solely those of the individual author(s) and contributor(s) and not of MDPI and/or the editor(s). MDPI and/or the editor(s) disclaim responsibility for any injury to people or property resulting from any ideas, methods, instructions or products referred to in the content.